Towards Complexity for Quantum Field Theory States

Shira Chapman,[1,*] Michal P. Heller,[2,†] Hugo Marrochio,[1,3,‡] and Fernando Pastawski[4,§]

[1] *Perimeter Institute for Theoretical Physics, Waterloo, Ontario N2L 2Y5, Canada*
[2] *Max Planck Institute for Gravitational Physics, Potsdam-Golm, D-14476, Germany*
[3] *Department of Physics & Astronomy and Guelph-Waterloo Physics Institute, University of Waterloo, Waterloo, ON N2L 3G1, Canada*
[4] *Dahlem Center for Complex Quantum Systems, Freie Universität Berlin, Berlin, D-14195, Germany*

We investigate notions of complexity of states in continuous quantum-many body systems. We focus on Gaussian states which include ground states of free quantum field theories and their approximations encountered in the context of the continuous version of Multiscale Entanglement Renormalization Ansatz. Our proposal for quantifying state complexity is based on the Fubini-Study metric. It leads to counting the number of applications of each gate (infinitesimal generator) in the transformation, subject to a state-dependent metric. We minimize the defined complexity with respect to momentum preserving quadratic generators which form $\mathfrak{su}(1,1)$ algebras. On the manifold of Gaussian states generated by these operations the Fubini-Study metric factorizes into hyperbolic planes with minimal complexity circuits reducing to known geodesics. Despite working with quantum field theories far outside the regime where Einstein gravity duals exist, we find striking similarities between our results and holographic complexity proposals.

1. Introduction.– Applications of quantum information concepts to high energy physics and gravity have recently led to many far-reaching developments. In particular, it has become apparent that special properties of entanglement in holographic [1] quantum field theories (QFT)s states are crucial for the emergence of smooth higher-dimensional (bulk) geometries in the gauge-gravity duality [2]. Much of the progress in this direction was achieved building on the holographic entanglement entropy proposal by Ryu and Takayanagi [3] which geometrizes the von Neumann entropy of a reduced density matrix of a QFT in a subregion in terms of the area of codimension-2 bulk minimal surfaces anchored at the boundary of this subregion (see e.g., Ref. [4] for a recent overview). However, Ryu-Takayanagi surfaces are often unable to access the whole holographic geometry [5–7]. This observation has led to significant interest in novel, from the point of view of quantum gravity, codimension-1 (volume) and codimension-0 (action) bulk quantities, whose behavior suggests conjecturing a link with the information theory notion of quantum state complexity [8–14]. In fact, a certain identification between complexity and action was originally suggested by Toffoli [15, 16] outside the context of holography.

Quantum state complexity originates from the field of quantum computations, which are usually modeled in a finite Hilbert space as the application of a sequence of gates chosen from a discrete set. In this context, the complexity of a unitary U is roughly associated with the minimal number of gates necessary to realize (or approximate) U. Notable progress has been made in connecting this notion to distance in Riemannian geometries derived from a set of generators [17]. The complexity of a target state $|T\rangle$ is usually subordinated to unitary complexity by specifying a "simple" reference state $|R\rangle$ and minimizing the complexity of U subject to $|T\rangle = U|R\rangle$ [18, 19].

In the context of holography, the organization of discrete tensor networks (seen as a quantum circuit U) has been suggested to give a qualitative picture of how quantum states give rise to emergent geometries [20]. This heuristic analysis was applied to the multiscale entanglement renormalization ansatz (MERA) [21], employed to find ground states of critical physical theories presenting a tensor network structure reminiscent of an AdS time slice. This motivated proposing "complexity equals volume" (CV) [9] and "complexity equals action" (CA) [11, 12] as new entries in the holographic dictionary. However, in holography one naturally considers continuum setups, QFTs, and there are shortcomings of traditional approaches to complexity when attempting to address field theory states. The aim of this letter is to bridge a pressing gap by exploring complexity-motivated distance measures in QFTs.

The main challenges in providing a workable definition of complexity in the continuum are related to choosing: a) a reference state $|R\rangle$, b) a set of allowed gates (correspondingly infinitesimal generators), c) a measure for how such gates contribute to the resulting distance function and a procedure for how to minimize it, d) a way to regulate ultraviolet (UV) divergences. Our proposed choice for c) is to measure the complexity by integrating the Fubini-Study (FS) line element along a path from $|R\rangle$ to $|T\rangle$ associated to an allowed realization of U. Minimizing the path will amount to studying geodesics on the manifold of quantum states induced by allowed generators acting on the reference state.[1]

[1] Another approach to complexity based on Ref. [17], is currently being pursued by R. Jefferson and R. Myers [22], see talks [23] for a preliminary outline of their results. See also [24–26] for a complexity proposal based on path integral optimization with

While this prescription is quite general, our choices for a), b) and d) render the necessary calculations tractable. Some of these choices, are inspired by the continuous MERA (cMERA) approach to free QFTs pioneered in Refs. [28–30], which we briefly review in [31]A. Similarly to the states in cMERA, our choices for the reference state $|R\rangle$ and target state $|T\rangle$ will be *pure Gaussian states* and allowed generators will be subsets of quadratic operators. We perform our analysis in momentum space and ignore frequencies above the UV cutoff Λ which equips us with a notion of approximation. As a first step, we consider the two mode squeezing operator for each pair of opposite momenta $\pm\vec{k}$. We then extend our analysis to include the full set of momentum preserving quadratic generators which form $\mathfrak{su}(1,1)$ algebras. In this case the study of minimal complexity reduces to the study of geodesics on a product of hyperbolic planes.

2. Complexity from the Fubini-Study metric.– We are interested in considering unitary operators U arising from iterating generators $G(s)$ taken from some elementary set of Hermitian operators $\mathcal{G}$. The allowed transformations U can then be represented as path ordered exponentials

$$U(\sigma) = \mathcal{P} e^{-i\int_{s_i}^{\sigma} G(s) ds}\,. \tag{1}$$

Here, s parameterizes progress along a path, starting at s_i and ending at s_f and $\sigma \in [s_i, s_f]$ is some intermediate value of s. The path-ordering $\mathcal{P}$ is required for non-commuting generators $G(s)$. We seek a path achieving $|T\rangle \approx U(s_f)|R\rangle$, where $(\approx)$ indicates that states coincide for momenta below a cutoff Λ. According to the Fubini-Study (FS) line element (see e.g., [32]),

$$ds_{FS}(\sigma) = d\sigma \sqrt{\left|\partial_\sigma |\Psi(\sigma)\rangle\right|^2 - \left|\langle\Psi(\sigma)|\,\partial_\sigma|\Psi(\sigma)\rangle\right|^2}\,, \tag{2}$$

the circuit length of a path going via states $|\Psi(\sigma)\rangle$ is

$$\ell(|\Psi(\sigma)\rangle) = \int_{s_i}^{s_f} ds_{FS}(\sigma)\,. \tag{3}$$

For the path traced by intermediate states $|\Psi(\sigma)\rangle = U(\sigma)|R\rangle$, where $U(\sigma)$ was given in Eq. (1), the line element of Eq. (3) reads

$$ds_{FS}(\sigma) = d\sigma \sqrt{\langle G^2(\sigma)\rangle_{\Psi(\sigma)} - \langle G(\sigma)\rangle^2_{\Psi(\sigma)}}\,, \tag{4}$$

and is independent of path reparametrizations.

If the path $|\Psi(\sigma)\rangle$ is unrestricted, the unique unitarily invariant distance measure $d_{R,T} = \arccos|\langle R \mid T\rangle| \leq \pi/2$ is obtained. However, by restricting the allowed generators $G(s)$, highly non-trivial notions of distance deserving the name complexity may be obtained. Our proposal is to define the complexity $\mathcal{C}$ as the minimal length according to Eq. (3) of a path from $|\Psi(s_i)\rangle \approx |R\rangle$ to $|\Psi(s_f)\rangle \approx |T\rangle$ driven by generators $G(s)$ in $\mathcal{G}$

$$\mathcal{C}(|R\rangle, |T\rangle, \mathcal{G}, \Lambda) = \min_{G(s)} \ell(|\Psi(\sigma)\rangle)\,. \tag{5}$$

The proposed complexity $\mathcal{C}$ inherits from the FS metric, the properties of a distance function. A key feature of the complexity given by Eq. (5) is that it remains well behaved even when $\mathcal{G}$ includes generators with unbounded norm (such as field operators).

While the definition of $\mathcal{C}$ is extremely general, even allowing arbitrary interacting field theories, we will only be able to evaluate it for very special parameters. It is only through appropriate choices of $\mathcal{G}$, $|R\rangle$ and $|T\rangle$, adapted to free QFTs, that the proposed complexity (5) becomes explicitly computable.

3. Gaussian states in free QFTs.– We will be considering a theory of free relativistic bosons in $(d+1)$-spacetime dimensions defined by the quadratic Hamiltonian

$$H_m = \int d^d x : \left\{ \frac{1}{2}\pi^2 + \frac{1}{2}(\partial_{\vec{x}}\phi)^2 + \frac{1}{2}m^2\phi^2 \right\} : \tag{6}$$

with commutation relations $[\phi(\vec{x}), \pi(\vec{x}')] = i\,\delta^d(\vec{x} - \vec{x}')$. This theory describes noninteracting particles created and annihilated by operators $a^\dagger_{\vec{k}}$ and $a_{\vec{k}}$ obeying $[a_{\vec{k}}, a^\dagger_{\vec{k}'}] = \delta^d(\vec{k} - \vec{k}')$. These are related to the field and momentum operators via $(\omega_k \equiv \sqrt{k^2 + m^2})$

$$\phi(\vec{k}) = \frac{1}{\sqrt{2\omega_k}}\left(a_{\vec{k}} + a^\dagger_{-\vec{k}}\right) \text{ and } \pi(\vec{k}) = \frac{\sqrt{\omega_k}}{\sqrt{2}i}\left(a_{\vec{k}} - a^\dagger_{-\vec{k}}\right) \tag{7}$$

and diagonalize the Hamiltonian: $H_m = \int d^d k\, \omega_k\, a^\dagger_{\vec{k}}\, a_{\vec{k}}$. For $m = 0$ we obtain a free *conformal field theory* (CFT).

A general translation invariant *pure Gaussian state* $|S\rangle$ is a state which is annihilated by generalized annihilation operators (nullifiers):

$$\left\{ \sqrt{\frac{\alpha_k}{2}}\phi(\vec{k}) + i\,\frac{1}{\sqrt{2\,\alpha_k}}\pi(\vec{k}) \right\} |S\rangle = 0\,, \tag{8}$$

with correlation functions in momentum space given by

$$\langle S|\phi(\vec{k})\phi(\vec{k}')|S\rangle = \frac{1}{2\,\alpha_k}\delta^{(d)}\left(\vec{k} + \vec{k}'\right). \tag{9}$$

The ground state $|m\rangle$ of the free theory (6), is a pure Gaussian state corresponding to $\alpha_k = \omega_k$. One can think of the ground state $|m\rangle$ as a product of vacuum states in momentum space in which for each momentum there are no particles according to the number operators $n_{\vec{k}} \equiv a^\dagger_{\vec{k}} a_{\vec{k}}$. In momentum space, the only nontrivial correlations in $|S\rangle$ are between $\vec{k}$ and $(-\vec{k})$ modes. In real-space, the $\vec{k}$-dependent factor on the RHS of Eq. (9) leads to spatial correlations (and entanglement).

Liouville action or [27] for a connection between complexity and randomness.

We adopt as a natural choice for a reference state $|R(M)\rangle$, the Gaussian state corresponding to

$$|R(M)\rangle : \qquad \alpha_k = M\,. \tag{10}$$

Since here α_k is independent of k this state is a product state with no spatial correlations, i.e., in real space the two point function of field operators takes the form $\langle R(M)|\phi(\vec{x})\phi(\vec{x}')|R(M)\rangle = \frac{1}{2M}\delta^d(\vec{x}-\vec{x}')$. Nevertheless in the basis associated with energy eigenstates of H_m momentum sectors $\vec{k}$ and $-\vec{k}$ are pairwise entangled according to (9). As we will see, the influence of the reference state scale M on complexity will be similar to the influence of certain ambiguities encountered in the context of holographic complexity. The annihilation and creation operators $b_{\vec{k}}$ and $b^\dagger_{\vec{k}}$ associated with the state $|R(M)\rangle$ can be written in terms of the creation and annihilation operators associated with the vacuum state $|m\rangle$, by means of a the following Bogoliubov transformation

$$\begin{aligned} &b_{\vec{k}} = \beta^+_k a_{\vec{k}} + \beta^-_k a^\dagger_{-\vec{k}}; \qquad b_{\vec{k}}|R(M)\rangle = 0; \\ &\beta^+_k = \cosh 2r_k; \quad \beta^-_k = \sinh 2r_k; \quad r_k \equiv \log\sqrt[4]{\frac{M}{\omega_k}}\,. \end{aligned} \tag{11}$$

As our target state we consider the approximate ground state $\left|m^{(\Lambda)}\right\rangle$ characterized by the UV momentum cut-off Λ. This approximate ground state is frequently used as starting point for the circuit in cMERA [28, 29], and corresponds to (see e.g. Ref. [33])

$$\left|m^{(\Lambda)}\right\rangle : \quad \alpha_k = \begin{cases} \omega_k, & k<\Lambda \ \ \text{(QFT vacuum)} \\ M, & k\geq\Lambda \ \ \text{(product state)} \end{cases}, \tag{12}$$

with correlation functions interpolating between those of the vacuum state $|m\rangle$ and the reference state $|R(M)\rangle$ as momentum increases according to Eq. (9). This state is in fact identical to the real ground state $|m\rangle$ up to the cut-off momentum.

The target states (12) can be reached from the reference states (10) by a circuit constructed with *two mode squeezing operators* which entangle the $\vec{k}$ and $-\vec{k}$ modes,

$$\begin{aligned} K(\vec{k}) &= \phi(\vec{k})\pi(-\vec{k}) + \pi(\vec{k})\phi(-\vec{k}) \\ &= i\left(a^\dagger_{\vec{k}}\,a^\dagger_{-\vec{k}} - a_{\vec{k}}\,a_{-\vec{k}}\right) = i\left(b^\dagger_{\vec{k}}\,b^\dagger_{-\vec{k}} - b_{\vec{k}}\,b_{-\vec{k}}\right). \end{aligned} \tag{13}$$

This operator is the main building block in cMERA circuits, and allows preparing the target state as

$$\left|m^{(\Lambda)}\right\rangle = e^{-i\int_{k\leq\Lambda} d^dk\, r_k\, K(\vec{k})}\,|R(M)\rangle \tag{14}$$

which is the starting point for our complexity analysis.

4. Ground state complexity with a single generator per pair of momenta $\pm\vec{k}$.– We start by evaluating our proposed complexity under the assumption that we allow for a single generator per pair of momenta $\pm\vec{k}$. As a concrete example we take $K(\vec{k})$ of Eq. (13), i.e., $\mathcal{G} = \mathsf{Span}\{K(\vec{k})\}$. In fact, in Sec. 6, we will prove that these generators achieve minimal complexity within a larger class of $\mathfrak{su}(1,1)$ generators. The circuits that we will consider in this section take the form (1) with $G(\sigma)$ given by

$$G(\sigma) = \int_{k\leq\Lambda} d^dk\, K(\vec{k}) y_{\vec{k}}(\sigma)\,. \tag{15}$$

Since all the $K(\vec{k})$ are commuting, the unitary $U(\sigma)$ of (1) is simply specified by the integrated values

$$Y_{\vec{k}}(\sigma) := \int_{s_i}^{\sigma} y_{\vec{k}}(s)ds; \qquad Y_{\vec{k}}(s_f) = r_k, \tag{16}$$

where $Y_{\vec{k}}(s_f)$ was fixed to match Eq. (14). The commutation of generators allows the variance associated to the line element (4) to be equivalently evaluated at any state $|\Psi(\sigma)\rangle$ along the path. Furthermore, the variance is additive with respect to the different $K(\vec{k})$ contributions because only equal or opposite momenta can be correlated. The complexity minimization of Eq. (5) then reduces to

$$\mathcal{C} = \min_{Y_{\vec{k}}(\sigma)} \int_{s_i}^{s_f} d\sigma \sqrt{2\,\mathrm{Vol}\int_{k\leq\Lambda} d^dk\,\left(\partial_\sigma Y_{\vec{k}}(\sigma)\right)^2}, \tag{17}$$

where $\mathrm{Vol}\equiv\delta^d(0)$ is the volume of the d-dimensional time slice. One recognizes a flat Euclidean geometry with coordinates $Y_{\vec{k}}(\sigma)$ continuously labeled by $\vec{k}$. To achieve minimal complexity the generators for the different momenta must act simultaneously with ratio dictated by Eq. (16) (straight path). A particularly simple affine parametrization for the path is

$$Y_{\vec{k}}(\sigma) = \frac{\sigma - s_i}{s_f - s_i}\, Y_{\vec{k}}(s_f); \quad y_k(\sigma) = \frac{1}{s_f - s_i}\, Y_{\vec{k}}(s_f). \tag{18}$$

As the corresponding cMERA circuit presents a σ dependent ratio, the complexity associated with it will be larger (as shown in [31]A). Evaluating (17) with (18), the minimal complexity reads

$$\mathcal{C}^{(2)} = \sqrt{2\,\mathrm{Vol}\int_{k\leq\Lambda} d^dk\, r_k^2}\,, \tag{19}$$

where the superscript (2) anticipates an interpretation of Eq. (19) as an L^2 norm.

Suppose on the other hand that $\mathcal{G}$ contains only individual generators $K(\vec{k})$ and not their linear span. This is analogous to disallowing different elementary gates in a circuit to act simultaneously. Our path parameters in this case consist of σ and $\vec{k}$. The arguments leading to Eq. (17) continue to hold except that now, the k integral must be pulled out of the square root and an extra $\sqrt{\mathrm{Vol}/2}$ factor appears. This leads to an L^1 norm (Manhattan distance) complexity

$$\mathcal{C}^{(1)} = \mathrm{Vol}\int_{k\leq\Lambda} d^dk\,|r_k|\,. \tag{20}$$

More generally, and without reference to the Fubini-Study metric, one can postulate the L^n norms as a measure of complexity

$$\mathcal{C}^{(n)} = 2\sqrt[n]{\frac{\text{Vol}}{2}\int_{k\leq\Lambda} d^dk\ |r_k|^n}. \tag{21}$$

5. Properties of the ground state complexities $\mathcal{C}^{(n)}$.– Here we analyze the properties of our complexity proposals (19)-(21). In particular we focus on the structure of divergences. As we will see in Sec. 8 these carry similarities to the results found for holographic complexity.

The leading divergence in the complexity measures $\mathcal{C}^{(n)}$ is proportional to $\text{Vol}^{1/n}\Lambda^{d/n}$ when $M=\Lambda$, and to $\text{Vol}^{1/n}\Lambda^{d/n}\log(M/\Lambda)$ when M and Λ are independent. The structure of subleading divergences depends on the interplay between m, M and Λ and we will analyze it in more detail for the $n=1$ and $n=2$ cases. For free CFTs ($m=0$) we obtain the following exact expressions

$$\begin{aligned}
\frac{\Gamma\left(\frac{d}{2}+1\right)}{\pi^{\frac{d}{2}}\Lambda^d\text{Vol}}\mathcal{C}^{(1)}_{CFT} &= \begin{cases} \left|\log\sqrt[4]{\frac{M}{\Lambda}}\right| + \frac{M^d}{2d\Lambda^d} - \frac{1}{4d}, & M<\Lambda \\ \left|\log\sqrt[4]{\frac{M}{\Lambda}}\right| + \frac{1}{4\,d}, & M\geq\Lambda \end{cases} \\
\frac{\Gamma\left(\frac{d}{2}+1\right)}{2\pi^{\frac{d}{2}}\Lambda^d\text{Vol}}\left(\mathcal{C}^{(2)}_{CFT}\right)^2 &= \left|\log\sqrt[4]{\frac{M}{\Lambda}}\right|^2 + \frac{\log\sqrt[4]{\frac{M}{\Lambda}}}{2d} + \frac{1}{8d^2}.
\end{aligned} \tag{22}$$

If we denote $M = e^{\gamma_M}\Lambda$, we see that the first terms in Eqs. (22) are indifferent to the sign of γ_M. The remainder is smaller for a given value of $|\gamma_M|$ when γ_M is negative and this leads to a smaller complexity. To understand this, note that for $M<\Lambda$ some $\vec{k}$-modes already begin with the right correlations with their $(-\vec{k})$-counterparts. So our minimal unitary transformation can act much more mildly in the vicinity of this locus in momentum space which leads to a reduced complexity. One can also consider the structure of divergences when the reference state is the CFT vacuum and the target state is the approximate vacuum of a free massive QFT. We address this question in [31]B.

6. Ground state complexity using $\mathfrak{su}(1,1)$ generators.– The unitary operator from Eq. (14) is not the only one that transforms $|R(M)\rangle$ into $\left|m^{(\Lambda)}\right\rangle$. While arbitrary generators in $\mathcal{G}$ would trivialize the FS complexity, to the FS distance, minimizing circuit length for commuting generators is similarly straightforward. Here, we extend our minimization to the most general algebra of momentum preserving quadratic operators. For every value of $\vec{k}$, the operators

$$K_+ = \frac{b^\dagger_{\vec{k}}b^\dagger_{-\vec{k}}}{2},\quad K_- = \frac{b_{\vec{k}}b_{-\vec{k}}}{2},\quad K_0 = \frac{b^\dagger_{\vec{k}}b_{\vec{k}} + b_{-\vec{k}}b^\dagger_{-\vec{k}}}{4}, \tag{23}$$

generate the $\mathfrak{su}(1,1)$ subalgebra of quadratic generators commuting with $n_{\vec{k}} - n_{-\vec{k}}$. Note that $K = 2i(K_+ - K_-)$ of Eq. (13) belongs to this algebra. Using the relevant decomposition formula, see e.g., [34] Appendix 11.3.3 and [31]C, one can establish that the following family of Hermitian operators

$$B(\vec{k},M) = -2\sinh(2r_k)[K_+ + K_-] + 4\cosh(2r_k)K_0, \tag{24}$$

can also be used (cf. (14)) to achieve the transformation

$$\left|m^{(\Lambda)}\right\rangle \equiv e^{-i\,\frac{\pi}{4}\int_{k\leq\Lambda} d^dk\, B\left(\vec{k},M\right)}|R(M)\rangle\,, \tag{25}$$

where $\equiv$ indicates equality up to an overall phase. In [31]D we minimize the circuit length subject to $\mathcal{G} = \mathsf{Span}\{B(\vec{k},M)\}$ proceeding as in Sec. 4 (see also Fig. 1 for an illustration of the generated path and a comparison to (14)).

The minimal circuit in Eqs. (1), (15) and (18) corresponds to the shortest path connecting the reference state $|R(M)\rangle$ to the approximate ground state $|m^{(\Lambda)}\rangle$ subject to $\mathcal{G} = \mathsf{Span}\{K(\vec{k})\}$. We will now consider paths generated by arbitrary combinations of the three momentum preserving generators spanning the $\mathfrak{su}(1,1)$ algebras in Eq. (23) (which include $K(\vec{k})$ and $B(\vec{k},M)$). We will see that the manifold of states generated by each $\mathfrak{su}(1,1)$ is a hyperbolic plane, one for each pair of momenta. Minimal complexity paths correspond to geodesic lines in the resulting tensor product manifold.

At the level of the state $|\Psi(\sigma)\rangle$, the most general $\mathfrak{su}(1,1)$ path can always be recast in the form (see [31]C)

$$|\Psi(\sigma)\rangle = \mathcal{N}e^{\int d^dk\gamma_+(\vec{k},\sigma)K_+(\vec{k})}|R(M)\rangle\,, \tag{26}$$

where $\mathcal{N}$ is a complex number and σ is the path parameter from Eq. (1). Normalization implies that up to an overall phase, the state depends only on γ_+. The existence of spurious parameters is a manifestation of the non uniqueness of the unitary achieving a minimal complexity path. At each point of the path, there is a subspace of generators consistent with minimal complexity. However, due to the non-commutative nature of the generators, there is a non-trivial relationship between them and $\gamma_+(\vec{k},\sigma)$. Our reference state $|R(M)\rangle$ corresponds to $\gamma_+(\vec{k},s_i)=0$ while the target state $\left|m^{(\Lambda)}\right\rangle$ corresponds to $\gamma_+(\vec{k},s_f) = \tanh(2r_k)$.

Evaluating the Fubini-Study line element (2) along the path (26) leads to the following remarkably simple form

$$ds_{FS}(\sigma) = d\sigma\sqrt{\frac{\text{Vol}}{2}\int_\Lambda d^d\vec{k}\frac{\gamma'_+(\vec{k},\sigma)\gamma'^*_+(\vec{k},\sigma)}{(1-|\gamma_+(\vec{k},\sigma)|^2)^2}}, \tag{27}$$

(see [31]C for the derivation). This line element corresponds to a direct product of Poincaré disks parameterized by the complex coordinates $\gamma_+(\vec{k}) = \gamma_+(-\vec{k})$ ($|\gamma_+(\vec{k})|<1$), one for each pair of momenta $\pm\vec{k}$ (an example of such a disk is illustrated in Fig. 1). The Poincaré disk is the manifold naturally associated with the coset $SU(1,1)/U(1)$ (see e.g., [35–37]) and its structure of geodesics is well known. Given an affinely parameterized geodesic on a Riemannian product manifold

such as (27), its natural projections are also affinely parameterized geodesics within each factor manifold. The relative speed of these projections are coupled and will, as in (18), be fixed by the target state.

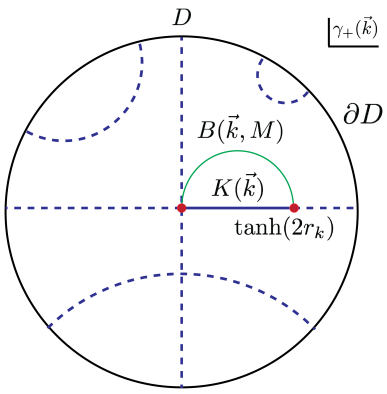

FIG. 1. The Poincaré disk, parameterized by real (horizontal) and imaginary (vertical) components of γ_+. Examples of geodesic lines appear in dashed blue. The two red dots indicate the reference state (the origin of the disc) and the target state (on the real axis). The geodesic connecting the two is the straight blue line along the diameter, corresponding to the generator $K(\vec{k})$. The green semicircle is the non-geodesic path generated by $B(\vec{k}, M)$ (see Eqs. (24)-(25) and [31]D). The $\mathfrak{su}(1,1)$ algebra generates isometries on the hyperbolic plane, with K_0 generating rotations around the origin and $K_1 \equiv \frac{K_+ + K_-}{2}$ and $K_2 \equiv \frac{K_+ - K_-}{2i}$ respectively being pure translations along the imaginary and real axes.

The geodesic connecting $|R(M)\rangle$ and $|m^{(\Lambda)}\rangle$ follows the radial direction on the Poincaré disc. This is precisely the affinely parameterized path $\gamma_+(\vec{k}, \sigma) = \tanh(2r_k\sigma)$, $\sigma \in [0, 1]$, generated by $K(\vec{k})$ of Sec. 4. This shows that the path described by Eqs. (15), (18) leads to minimal complexity even within the larger class of $\mathfrak{su}(1,1)$ generators.

8. Comparison with Holographic Complexity Proposals.– Let us now comment on the relation between the leading divergences in Eq. (22), and holography. Currently there are two proposals for the gravity dual of complexity in terms of maximal codimension-1 volumes in the dual spacetime geometry (complexity = volume, CV [9]) or on-shell bulk actions evaluated in the so-called Wheeler-DeWitt patch bounded by null hypersurfaces in the bulk spacetime (complexity = action, CA [11, 12]). The structure of the vacuum UV divergences of complexity for both conjectures can be characterized by a UV regularization scheme [13, 14, 38] with the cut-off distance from the AdS boundary in Fefferman-Graham coordinates identified as $\delta \sim 1/\Lambda$. Our analysis in Eq. (22) for the L^1 norm indicates a leading divergence of $\mathrm{Vol}\,\Lambda^d \left|\log \frac{M}{\Lambda}\right|$, which resembles the result of the CA proposal. For the CFT, we saw that the subleading divergences except for $\mathrm{Vol}\,\Lambda^d$ and a constant vanish. This is similar to what happens in the CA proposals when curvature invariants over the relevant time slice vanish. In the holographic CA calculation, the leading logarithmic divergence is due to the codimension-2 joint action contributions associated with the intersection between the null and timelike hypersurfaces that bound the regulated Wheeler-DeWitt patch near the AdS boundary [39]. These contributions depend on the parametrization of null normals (e.g., [39] suggested working in an affine parametrization) and their overall rescaling. The latter gives rise to an extra freedom represented in [13] by a free parameter $\tilde{\alpha}$ inside the logarithm. In our calculation the same type of ambiguity is related to the choice of the reference state scale M. In fact we can identify $M \sim \tilde{\alpha}/L_{\mathrm{AdS}}$ where L_{AdS} is the AdS scale. When $M = \omega_\Lambda$, the leading divergence becomes proportional to $\mathrm{Vol}\,\Lambda^d$, which is in agreement with the CV conjecture results [13]. Furthermore, if we include a certain counterterm in the Einstein-Hilbert action leading to a reparametrization invariant action, the leading divergence in the CA proposal also becomes equal to $\mathrm{Vol}\,\Lambda^d$ [38]. On the contrary, none of the holographic proposals have a structure of divergences as in Eq. (22) for the L^2 norm and of those described in [31] B and D. It is interesting that even though we considered QFTs without semiclassical gravity duals (having small central charge and no interactions), the L^1 norm analyzed in Eq. (22) exhibits close similarity to the holographic calculations of leading UV divergences.

9. Summary and Outlook.– In this letter, we proposed a definition of state complexity applicable to the setting of QFTs. This measure can be derived from the Fubini-Study metric by restricting to directions permitted by allowed generators $\mathcal{G}$, on which our measure crucially depends. We identified a set of unitary paths that map simple Gaussian reference states $|R(M)\rangle$ with no spatial entanglement to approximate ground states (faithful up to momenta $k > \Lambda$) of free QFTs, generated within an $\mathfrak{su}(1,1)$ subalgebra of momentum preserving quadratic generators. Among these paths, we singled out those corresponding to minimal complexity according to our measure. Remarkably, for some instances, the evaluated complexity presents qualitative agreement with holographic results. In forthcoming work [40], we will analyze thermofield double states in free QFTs and their time evolution providing further ground for comparison with holography. Further crosschecks with holography include evaluating our complexity proposals for fermionic systems and verifying whether, as in holography, they are proportional to the central charge. Finally, we expect further insights may be gained on the role of locality in complexity by evaluating our state complexity with respect to (bi)local elementary generators in real space. The cMERA approach of Ref. [33] seems like a good starting point for such future investigations.

We would like to thank G. Verdon-Akzam, J. de Boer, P. Caputa, M. Fleury, A. Franco, K. Hashimoto, Q. Hu, R. Janik, J. Jottar, T. Osborne, G. Policastro, K. Rejzner, D. Sarkar, V. Scholz, M. Spalinski, T. Takayanagi, K. Temme, J. Teschner, G. Vidal, F. Verstraete and P. Witaszczyk for valuable comments and discussions. We are particularly thankful to J. Eisert for numerous comments on this work and to R. Myers and R. Jefferson for illuminating discussions, for sharing their results [22, 23] on defining complexity in QFTs using Nielsen's geometry [17] and for suggesting to vary the reference state scale M. Research at Perimeter Institute is supported by the Government of Canada through Industry Canada and by the Province of Ontario through the Ministry of Research & Innovation. S.C. acknowledges additional support from an Israeli Women in Science Fellowship from the Israeli Council of Higher Education. The research of M.P.H. is supported by the Alexander von Humboldt Foundation and the Federal Ministry for Education and Research through the Sofja Kovalevskaja Award. M.P.H is also grateful to Perimeter Institute, ETH and the University of Amsterdam for stimulating hospitality during the completion of this project and to Kyoto University where this work was presented for the first time during the workshop *Quantum Gravity, String Theory and Holography* in April 2017. F.P. would also like to acknowledge the support of the Alexander von Humboldt Foundation.

* schapman@perimeterinstitute.ca
† michal.p.heller@aei.mpg.de; aei.mpg.de/GQFI;
On leave from: *National Centre for Nuclear Research, 00-681 Warsaw, Poland.*
‡ hmarrochio@perimeterinstitute.ca
§ fernando.pastawski@gmail.com

[1] J. M. Maldacena, Int. J. Theor. Phys. **38**, 1113 (1999), [Adv. Theor. Math. Phys.2,231(1998)], arXiv:hep-th/9711200 [hep-th].
[2] M. Van Raamsdonk, Gen. Rel. Grav. **42**, 2323 (2010), [Int. J. Mod. Phys.D19,2429(2010)], arXiv:1005.3035 [hep-th].
[3] S. Ryu and T. Takayanagi, Phys. Rev. Lett. **96**, 181602 (2006), arXiv:hep-th/0603001 [hep-th].
[4] M. Rangamani and T. Takayanagi, (2016), arXiv:1609.01287 [hep-th].
[5] V. Balasubramanian, B. D. Chowdhury, B. Czech, and J. de Boer, JHEP **01**, 048 (2015), arXiv:1406.5859 [hep-th].
[6] L. Susskind, Fortsch. Phys. **64**, 49 (2016), arXiv:1411.0690 [hep-th].
[7] B. Freivogel, R. A. Jefferson, L. Kabir, B. Mosk, and I.-S. Yang, Phys. Rev. **D91**, 086013 (2015), arXiv:1412.5175 [hep-th].
[8] L. Susskind, Fortsch. Phys. **64**, 24 (2016), arXiv:1403.5695 [hep-th].
[9] D. Stanford and L. Susskind, Phys. Rev. **D90**, 126007 (2014), arXiv:1406.2678 [hep-th].
[10] M. Alishahiha, Phys. Rev. **D92**, 126009 (2015), arXiv:1509.06614 [hep-th].
[11] A. R. Brown, D. A. Roberts, L. Susskind, B. Swingle, and Y. Zhao, Phys. Rev. Lett. **116**, 191301 (2016), arXiv:1509.07876 [hep-th].
[12] A. R. Brown, D. A. Roberts, L. Susskind, B. Swingle, and Y. Zhao, Phys. Rev. **D93**, 086006 (2016), arXiv:1512.04993 [hep-th].
[13] D. Carmi, R. C. Myers, and P. Rath, JHEP **03**, 118 (2017), arXiv:1612.00433 [hep-th].
[14] S. Chapman, H. Marrochio, and R. C. Myers, JHEP **01**, 062 (2017), arXiv:1610.08063 [hep-th].
[15] T. Toffoli, Physica D: Nonlinear Phenomena **120**, 1 (1998).
[16] T. Toffoli, in *Feynman and computation : exploring the limits of computers*, edited by A. J. G. Hey and R. P. Feynman (Perseus Books, 1999) pp. 349–392.
[17] M. A. Nielsen, M. R. Dowling, M. Gu, and A. C. Doherty, Science **311** (2006).
[18] J. Watrous, ArXiv e-prints (2008), arXiv:0804.3401 [quant-ph].
[19] S. Aaronson (2016) arXiv:1607.05256 [quant-ph].
[20] B. Swingle, Physical Review D **86**, 065007 (2012).
[21] G. Vidal, Phys. Rev. Lett. **101**, 110501 (2008).
[22] R. A. Jefferson and R. C. Myers, *forthcoming: Circuit complexity in quantum field theory*.
[23] R. C. Myers, "Complexity, holography & quantum field theory," (2017), Pirsa: 17040050, see also Strings 2017 conference.
[24] P. Caputa, N. Kundu, M. Miyaji, T. Takayanagi, and K. Watanabe, (2017), arXiv:1703.00456 [hep-th].
[25] P. Caputa, N. Kundu, M. Miyaji, T. Takayanagi, and K. Watanabe, (2017), arXiv:1706.07056 [hep-th].
[26] B. Czech, (2017), arXiv:1706.00965.
[27] D. A. Roberts and B. Yoshida, Journal of High Energy Physics **2017**, 121 (2017).
[28] J. Haegeman, T. J. Osborne, H. Verschelde, and F. Verstraete, Phys. Rev. Lett. **110**, 100402 (2013), arXiv:1102.5524 [hep-th].
[29] M. Nozaki, S. Ryu, and T. Takayanagi, JHEP **10**, 193 (2012), arXiv:1208.3469 [hep-th].
[30] A. Mollabashi, M. Nozaki, S. Ryu, and T. Takayanagi, JHEP **03**, 098 (2014), arXiv:1311.6095 [hep-th].
[31] Supplementary material, composed of five sections. In section A, we evaluate the length of the path traced by the cMERA circuit according to the Fubini-Study metric. In section B, we consider a lower bounded constant generator which induces constant period oscillations between the reference and target states and evaluate the corresponding Fubini-Study length. In section C, we evaluate the complexity of massive field theory ground states with respect to the CFT vacuum state. In section D, we provide further details on how the hyperbolic planes can be identified in the manifold induced by the $\mathfrak{su}(1,1)$ algebras. In section E we present a simplified derivation of the hyperbolic plane metric for a single pair of modes.
[32] I. Bengtsson and K. Zyczkowski, *Geometry of Quantum States: An Introduction to Quantum Entanglement* (Cambridge University Press, 2007).
[33] Q. Hu and G. Vidal, (2017), arXiv:1703.04798 [quant-ph].
[34] A. B. Klimov and S. M. Chumakov, *A group-theoretical approach to quantum optics : models of atom-field inter-*

actions (Wiley-VCH, 2009) p. 322.
[35] A. M. Perelomov, Commun. Math. Phys. **26**, 222 (1972).
[36] J. P. Provost and G. Vallee, Commun. Math. Phys. **76**, 289 (1980).
[37] A. M. Perelomov, *Generalized coherent states and their applications* (1986).
[38] A. Reynolds and S. F. Ross, Class. Quant. Grav. **34**, 105004 (2017), arXiv:1612.05439 [hep-th].
[39] L. Lehner, R. C. Myers, E. Poisson, and R. D. Sorkin, Phys. Rev. **D94**, 084046 (2016), arXiv:1609.00207 [hep-th].
[40] S. Chapman, M. P. Heller, R. A. Jefferson, H. Marrochio, R. C. Myers, and F. Pastawski, *in preparation*.

A. cMERA circuit length according to the Fubini-Study metric

Here, we evaluate the cMERA circuit length according to the proposed Fubini-Study metric. We demonstrate that in the $\mathcal{C}^{(2)}$ norm, the cMERA circuit is longer (i.e., more complex) than the minimal circuit described in Sec. 4 whereas in the $\mathcal{C}^{(1)}$ norm its circuit length coincides with the corresponding minimal complexity. We review below the needed ingredients of cMERA and refer the reader to Ref. [28–30] for extra details.

cMERA is a unitary map taking the Gaussian reference state $|R(M)\rangle$ defined by Eqs. (8) and (10), which is a product state with no spatial correlations, to the approximate ground state $\left|m^{(\Lambda)}\right\rangle$ given by Eqs. (8) and (12). One can view $|R(M)\rangle$ as the ground state of an *ultra-local Hamiltonian*

$$H_M = \int d^d x : \left\{\pi^2 + M^2\phi^2\right\}/2 :, \tag{28}$$

where the $(\partial_{\vec{x}}\phi)^2$ term is omitted and the mass M is kept arbitrary. Despite being a product state in real space, $|R(M)\rangle$ contains pairwise-entanglement in momentum space between momentum sectors $\vec{k}$ and $-\vec{k}$.

The cMERA circuit alters correlation between the $\vec{k}$ and $-\vec{k}$ modes from those corresponding to a constant and set by M to the ones governed by α_k of Eq. (12) in a scale (i.e., u) dependent manner as follows

$$\left|m^{(\Lambda)}\right\rangle = \mathcal{P}\, e^{-\frac{i}{2}\int_{-\infty}^{0} du \int_{k\le\Lambda e^u} d^d k\, K(\vec{k})\,\chi(u)}\, |R(M)\rangle\,. \tag{29}$$

The two mode squeezing operator $K(\vec{k})$ defined in Eq. (13) (dis)entangles the $\vec{k}$ and $-\vec{k}$ modes along the circuit. Energy minimization w.r.t. the free Hamiltonian H_m implies

$$\chi(u) = \frac{1}{2}\frac{e^{2u}}{e^{2u} + m^2/\Lambda^2} \text{ and } M = \omega_\Lambda \equiv \sqrt{\Lambda^2 + m^2}. \tag{30}$$

Comparing with Eq. (1) we see that the renormalization-group scale parameter u running from the infrared at $u = -\infty$ to the ultraviolet at $u = 0$ plays the role of $\sigma \in [s_i, s_f]$ and $\int_{k\le\Lambda e^u} d^d\vec{k} K(\vec{k})\chi(u)/2$ is equivalent to $G(s)$. We also note that for every value of u, the action of the circuit on momenta larger than Λe^u is suppressed. Since the operators $K(\vec{k})$ all commute, we may integrate over u in Eq. (29) to obtain

$$\left|m^{(\Lambda)}\right\rangle = e^{-i\int_{k\le\Lambda} d^d k\, K(\vec{k})\, \log\sqrt[4]{\frac{\omega_\Lambda}{\omega_k}}}\, |R(\omega_\Lambda)\rangle. \tag{31}$$

The above expression is the cMERA realization of Eq. (14).

Evaluating the Fubini-Study metric distance according to Eq. (3) for the cMERA circuit yields

$$\ell^{(2)}_{\text{cMERA}} = \int_{-\infty}^{0} du\,\chi(u)\sqrt{\frac{\text{Vol}}{2}\int_{k<\Lambda e^u} d^d k}. \tag{32}$$

We can evaluate this expression analytically and obtain

$$\frac{\Gamma\left(\frac{d}{2}+1\right)(\ell^{(2)}_{\text{cMERA}})^2}{2\pi^{d/2}\text{Vol}\,\Lambda^d} = \frac{\Lambda^4\, {}_2F_1\left(1, \frac{d+4}{4}; \frac{d+8}{4}; -\frac{\Lambda^2}{m^2}\right)^2}{4(d+4)^2 m^4}, \tag{33}$$

where for the massless theory, the expression simplifies

$$\frac{\Gamma\left(\frac{d}{2}+1\right)}{2\pi^{d/2}\text{Vol}\,\Lambda^d}\left(\ell^{(2)}_{\text{cMERA}}\right)^2\Big|_{m=0} = \frac{1}{4d^2}\,. \tag{34}$$

This is equivalent to the complexity $\mathcal{C}^{(2)}$ of Eq. (19). Comparing to the relevant entry in Eq. (22) we conclude that the path generated by cMERA is a $\sqrt{2}$ longer than the minimal path associated with $K(\vec{k})$, studied in Sec. 4. Fig. 2 highlights the differences between these two circuits.

If we now disallow the different elementary generators in the cMERA circuit to act simultaneously and consider the equivalent of the $\mathcal{C}^{(1)}$ norm, we end up with

$$\ell^{(1)}_{\text{cMERA}} = \frac{\text{Vol}}{2}\int_{-\infty}^{0} du\,\chi(u)\int_{k<\Lambda e^u} d^d k, \tag{35}$$

which yields precisely the same circuit length as the one obtained in Eq. (20). This is due to the fact that the $\mathcal{C}^{(1)}$ norm is invariant under independent reparametrizations of the circuits associated with the different pairs of momenta.

B. Complexity starting with the CFT vacuum

Here, we evaluate the complexity of the ground state of a massive QFT starting with a different reference state, namely instead of considering $|R(M)\rangle$ as our reference state, we will consider the vacuum of a free CFT $|0\rangle$ ($m = 0$). The transformation between $|0\rangle$ and $\left|m^{(\Lambda)}\right\rangle$ takes the form

$$\left|m^{(\Lambda)}\right\rangle = e^{-i\int_{k\le\Lambda} d^d k\, \bar{r}_k K(\vec{k})}|0\rangle; \quad \bar{r}_k \equiv \log\sqrt[4]{\frac{|\vec{k}|}{\omega_k}}\,. \tag{36}$$

For the physically interesting case $\Lambda \gg m$, we see that the parameter of the transformation, $\bar{r}_k$, at large momenta approaches 0 in accord with the physical intuition that mass becomes irrelevant in the UV. However, this does not mean that the complexity of the transformation does not diverge with the cut-off due to the growth of the number of momentum modes in the UV. Adapting the $n = 1$ instance of our complexity proposal given by Eq. (20) to the present case, i.e., replacing the $r_k \equiv \log \sqrt[4]{M/\omega_k}$ by $\bar{r}_k \equiv \log \sqrt[4]{|\vec{k}|/\omega_k}$, we obtain that the complexity is now finite for $d = 1$, diverges logarithmically with the cut-off, $(m^2\text{Vol}) \log \frac{\Lambda}{m}$, for $d = 2$ and in higher number of dimensions behaves as $(m^d\text{Vol}) \left(\frac{\Lambda}{m}\right)^{d-2}$, for large values of the cutoff. This behavior is subleading w.r.t. Eq. (22) valid for starting with the unentangled reference state. What we thus see is that taking the ground state of another QFT as a reference state significantly lowers the complexity of the transformation needed to obtain $\left|m^{(\Lambda)}\right\rangle$, cf. Eq. (22), since some of the correlations have already been built, but still leads to UV-divergent results in space dimensions $d > 1$.

C. $\mathfrak{su}(1,1)$ manifold – metric and geodesics

Here, we provide the detailed derivation of the results of Sec. 6. In particular we study the general form of the manifold of states generated by the elements of $\mathfrak{su}(1,1)$ (23), and the metric and geodesics induced on this manifold by the Fubini-Study metric.

A path in the manifold of states will correspond to a path ordered exponential of the various $\mathfrak{su}(1,1)$ elements. For every point in the path such an exponent can always be regrouped as

$$|\Psi(\sigma)\rangle = U(\sigma)|R(M)\rangle; \qquad U(\sigma) \equiv e^{\int_\Lambda d^d k\, g(\vec{k},\sigma)}\,, \quad (37)$$

where

$$\begin{aligned} g(\vec{k},\sigma) =& \alpha_+(\vec{k},\sigma)K_+(\vec{k}) \\ &+ \alpha_-(\vec{k},\sigma)K_-(\vec{k}) + \omega(\vec{k},\sigma)K_0(\vec{k}), \end{aligned} \quad (38)$$

and σ is the path parameter from Eq. (1). This is due to the fact that the $\mathfrak{su}(1,1)$ generators form a closed algebra. The coefficients $\alpha_\pm(\vec{k},\sigma)$ and $\omega(\vec{k},\sigma)$ are not simply related to the original coefficients of the various generators in the path ordered trajectory (1) because of the noncommutative nature of generators. Unitarity implies that $\alpha_+^*(\sigma) = -\alpha_-(\sigma)$ and $\omega^*(\sigma) = -\omega(\sigma)$.

The unitary (38) can then be decomposed as follows (see e.g., [34] Appendix 11.3.3):

$$\begin{aligned} U(\sigma) =& e^{\int_\Lambda d^d k \gamma_+(\vec{k},\sigma)K_+(\vec{k})} \times \\ & e^{\int_\Lambda d^d k \log\gamma_0(\vec{k},\sigma)K_0(\vec{k})} e^{\int_\Lambda d^d k \gamma_-(\vec{k},\sigma)K_-(\vec{k})}\,, \end{aligned} \quad (39)$$

where the mapping between the coefficients is

$$\begin{aligned} \gamma_\pm =& \frac{2\,\alpha_\pm \sinh\Xi}{2\,\Xi\cosh\Xi - \omega\sinh\Xi}\,, \\ \gamma_0 =& \left(\cosh\Xi - \frac{\omega}{2\Xi}\sinh\Xi\right)^{-2}\,, \\ \Xi^2 \equiv& \frac{\omega^2}{4} - \alpha_+\alpha_-\,. \end{aligned} \quad (40)$$

Note that unitarity implies that $|\gamma_+| < 1$, which fits nicely into the geometric picture describing the γ_+ manifold as a Poincaré *unit* disk. We can now use the identities

$$K_-|R(M)\rangle = 0; \quad K_0|R(M)\rangle = \frac{\delta^{(d)}(0)}{4}|R(M)\rangle. \quad (41)$$

to get rid of the information contained in the path parameters which do not change our state, or only change it up to an overall phase. This can be done by showing that the state in Eq. (39) can be recast as

$$\begin{aligned} |\Psi(\sigma)\rangle =& \mathcal{N} e^{\int_\Lambda d^d k \gamma_+(\vec{k},\sigma)K_+(\vec{k})}|R(M)\rangle\,, \\ \mathcal{N} =& e^{\frac{\delta^{(d)}(0)}{4}\int_\Lambda d^d k \log\gamma_0(\vec{k},\sigma)}\,, \end{aligned} \quad (42)$$

where $\mathcal{N}$ is a complex constant containing information about the overall normalization and phase. The identity $|\gamma_0| = 1 - |\gamma_+|^2$ allows to demonstrate that up to an unphysical overall phase, the state depends only on γ_+.

One can then use the following set of adjoint conjugation identities to evaluate the Fubini-Study line element along the path (42)

$$\begin{aligned} & e^{\int_\Lambda d^d k' \lambda(\vec{k}',\sigma)K_+(\vec{k}')} K_0(\vec{k}) e^{-\int_\Lambda d^d k' \lambda(\vec{k}',\sigma)K_+(\vec{k}')} \\ &\quad = K_0(\vec{k}) - K_+(\vec{k})\lambda(\vec{k},\sigma)\,, \\ & e^{\int_\Lambda d^d k' \lambda(\vec{k}',\sigma)K_-(\vec{k}')} K_+(\vec{k}) e^{-\int_\Lambda d^d k' \lambda(\vec{k}',\sigma)K_-(\vec{k}')} \\ &\quad = K_+(\vec{k}) + 2\lambda(\vec{k},\sigma)K_0(\vec{k}) + \lambda(\vec{k},\sigma)^2 K_-(\vec{k})\,. \end{aligned} \quad (43)$$

This leads to a remarkably simple form, resulting in the following expression for the complexity

$$\mathcal{C} = \min_{\gamma_+(\vec{k},\sigma)} \int_{s_i}^{s_f} d\sigma \sqrt{\frac{\text{Vol}}{2}\int_\Lambda d^d\vec{k}\, \frac{\gamma_+'(\vec{k},\sigma)\gamma_+'^*(\vec{k},\sigma)}{(1-|\gamma_+(\vec{k},\sigma)|^2)^2}}, \quad (44)$$

where the prime denotes differentiation with respect to the path parameter σ. We identify the line element of a manifold which consists of a direct product of hyperbolic unit discs, one for each pair of momenta with γ_+ for the different momenta playing the role of the complex coordinates on the discs. The Poincaré unit disk, is known to be the manifold associated with the coset $SU(1,1)/U(1)$ (see e.g., [35–37]). However note that the form (27) couples the different speeds associated to the paths for different values of the momentum.

As explained in Sec. 6, affinely parameterized geodesic paths on the product space correspond to affinely parameterized geodesics in each one of the spaces, where the relative speeds for the paths of the different momenta are dictated by the requirement that we reproduce the target state $\gamma_+ = \tanh(2r_k)$ at the end of the path ($\sigma = s_f$). The geodesics on the Poincaré disk are well known in the literature and we identify the one connecting our reference state $\gamma_+ = 0$ to the target state as the blue line lying along the diameter in Fig. 1.

The paths generated by $K(\vec{k})$ in Eqs. (1), (15) and (18) and $B(\vec{k}, M)$ in Eq. (25) can be decomposed according to (37)-(40) as follows

$$\begin{aligned} K(\vec{k}): \qquad & \alpha_\pm(\vec{k},\sigma) = \pm 2 r_k \sigma, \quad \omega(\vec{k},\sigma) = 0\,, \\ & \gamma_+(\vec{k},\sigma) = \tanh(2 r_k \sigma)\,, \end{aligned} \tag{45}$$

and

$$\begin{aligned} B(\vec{k},M): & \\ \alpha_\pm(\vec{k},\sigma) =& \frac{i\pi}{2}\sinh(2r_k)\sigma\,, \\ \omega(\vec{k},\sigma) =& -i\pi\cosh(2r_k)\sigma\,, \\ \gamma_+(\vec{k},\sigma) =& \frac{i\sinh(2r_k)\sin(\frac{\pi\sigma}{2})}{\cos(\frac{\pi\sigma}{2}) + i\cosh(2r_k)\sin(\sigma\frac{\pi}{2})}\,, \end{aligned} \tag{46}$$

where here we have taken $\sigma \in [0,1]$. It is then possible to confirm that the path generated by $K(\vec{k})$ is an affinely parameterized geodesic according to Eq. (44) while the one generated by $B(\vec{k}, M)$ is not a geodesic as it does not satisfy the Euler Lagrange equations derived from Eq. (44).

For completeness we also specify the path corresponding to the cMERA circuit (see [31]A). After integrating the circuit (here it is possible since the generators commute) and decomposing according to Eq. (40) we obtain:

$$\gamma_+(\vec{k},\sigma) = \tanh\left[\frac{1}{4}\log\left[\frac{m^2+\sigma^2\Lambda^2}{k^2+m^2}\right]\right]\theta\left(\sigma - \frac{|k|}{\Lambda}\right), \tag{47}$$

where we have redefined the cMERA parameter $\sigma \equiv e^u$. Fig. 2 is a comparison of the minimal path (45) and the cMERA path (47). It presents γ_+ as a function of $\vec{k}$ for different values of σ and demonstrates in this way the progress of the circuit.

D. Another constant generator

What might be viewed as a deficiency of the transformation (14) adopted from cMERA is that its generators $K(\vec{k})$, see Eq. (13), do not have a spectrum bounded from below. As such, they cannot be naturally interpreted as Hamiltonians of some fiducial physical system. This is not the case for the generator $B(\vec{k}, M)$ of Eq. (24), which does admit an interpretation as a lower bounded

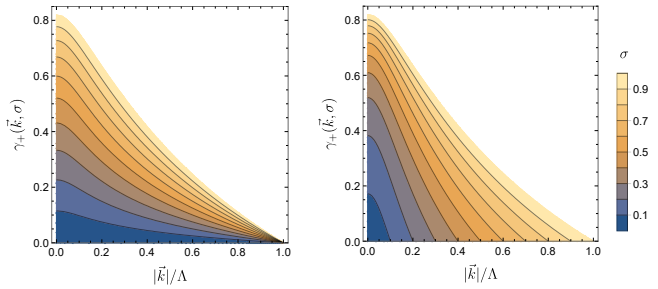

FIG. 2. Graphical description of the minimal circuit (45) (left) and the cMERA circuit (47) (right). The plots present γ_+ as a function of $|\vec{k}|/\Lambda$ for different values of σ represented by the different colored contours. We see that while the cMERA circuit only acts on momenta $|k|/\Lambda < \sigma$, the minimal circuit alters γ_+ for all the different momenta at every step of the circuit. In this plot we have chosen $m/\Lambda = 0.1$.

Hamiltonian. Below, we evaluate the path length associated with the generator $B(\vec{k}, M)$.

As mentioned at the end of Sec. 3, the approximate ground state $|m^{(\Lambda)}\rangle$ of Eq. (12) can also be reached, up to an overall phase, starting from the reference state $|R(M)\rangle$ of Eq. (10) by repeatedly applying the operator

$$B(\vec{k},M) = -2\sinh(2r_k)[K_+ + K_-] + 4\cosh(2r_k)K_0. \tag{48}$$

Indeed, using the relevant decomposition formulas Eqs. (37)-(40) (see e.g., [34]), one can establish that

$$\left|m^{(\Lambda)}\right\rangle \equiv e^{-i\frac{\pi}{4}\int_{k\le\Lambda} d^dk\, B(\vec{k},M)}|R(M)\rangle\,, \tag{49}$$

where $\equiv$ indicates that the states are equal up to an irrelevant global phase. Another way to obtain this transformation is to derive it using the properties of the Wigner distribution and we will describe it in detail in an upcoming publication [40]. It is interesting to note that in contrast to Eq. (14) the generators in Eq. (48) explicitly depend on both reference and target states. However, the number of times each of them is applied in Eq. (49) is fixed and equal to $\pi/4$. Generalizing Eq. (21) to the present case, we obtain for the different L^n norms

$$\mathcal{C}^{(n)} = \frac{\pi}{4}\sqrt[n]{\frac{\mathrm{Vol}}{2}\int_{k\le\Lambda} d^dk\left|\sqrt{M/\omega_k} - \sqrt{\omega_k/M}\right|^n}, \tag{50}$$

which reads at leading order in Λ:

$$\begin{aligned} &\frac{2^{2n+1}\Gamma\left(\frac{d}{2}+1\right)\left(\mathcal{C}^{(n)}\right)^n}{\pi^{\frac{d}{2}+n}\,\Lambda^d\,\mathrm{Vol}} \\ &= \begin{cases} \frac{2d}{2d+n}\left(\frac{\Lambda}{M}\right)^{n/2} + \ldots, & M \ll \Lambda, \\ \frac{2d}{2d-n}\left(\frac{M}{\Lambda}\right)^{n/2} + \ldots, & M \gg \Lambda,\ 2d > n. \end{cases} \end{aligned} \tag{51}$$

One can clearly see that the leading divergences at large UV cut-off Λ got now altered compared to those of Sec. 5 from $\Lambda^{\frac{d}{n}}$ to $\Lambda^{\frac{d}{n}\pm\frac{1}{2}}$ depending on the reference state scale

M. Notice also that for $M \ll \Lambda$ ($M \gg \Lambda$), the number of gates $K(\vec{k})$ needed for the transformation from $|M\rangle$ to $|m^{(\Lambda)}\rangle$ is smaller than the number of needed $B(M,\vec{k})$ gates. This is in line with our predictions of Sec. 6 since $B(\vec{k},M)$ deviates from the geodesic path generated by $K(\vec{k})$.

To make this statement more precise, let us study the length of the minimal path constructed with the generator $B(\vec{k},M)$ embedded inside the larger manifold spanned by the $\mathfrak{su}(1,1)$ generators (23)

$$|\Psi(\sigma)\rangle \equiv e^{-i\,\sigma\,\frac{\pi}{4}\int_{k\leq\Lambda} d^dk\, B(\vec{k},M)}|R(M)\rangle. \tag{52}$$

This path can be shown to be minimal when only $B(\vec{k},M)$ gates are allowed using the techniques of Sec. 4. According to the decomposition in Eqs. (37)-(40) we can show that this path corresponds to (see [31]C)

$$\gamma_+(\vec{k},\sigma) = \frac{i\sinh(2r_k)\sin(\sigma\frac{\pi}{2})}{\cos(\frac{\pi}{2}\sigma)+i\cosh(2r_k)\sin(\sigma\frac{\pi}{2})}\,. \tag{53}$$

Checking the Euler Lagrange equations explicitly for this path one concludes that it is not a geodesic. The path corresponding to $B(\vec{k},M)$ is represented in Fig. 1 by a green line. It would be interesting to explore if the operators $B(M,\vec{k})$ can lead to an alternative construction for a cMERA circuit.

E. Fubini-Study metric derivation for a single $\mathfrak{su}(1,1)$

Here, we present an alternative, simpler, derivation of Eq. (44) for a single pair of momenta. For this purpose, in the commutation relations of creation and annihilation operators, Dirac delta functions will be replaced by Kronecker deltas and integrals will be suppressed. We will restore them at the end of the calculation. We will consider states of the form

$$|\Psi(\sigma)\rangle = \mathcal{N}e^{\gamma_+ K_+}|0,0\rangle\,, \tag{54}$$

where the state $|0,0\rangle$ contains no particle excitation in the $\vec{k}$ and $-\vec{k}$ modes according to the annihilation operators $b_{\vec{k}}$. In fact the state $|R(M)\rangle$ is a product of such states $|0,0\rangle$ in the different momentum sectors. We can rewrite the state $|\Psi(\sigma)\rangle$ up to an overall phase as follows:

$$|\Psi(\sigma)\rangle \equiv \sqrt{1-|\gamma_+|^2}\sum_{n=0}^{\infty}(\gamma_+)^n\,|n,n\rangle\,, \tag{55}$$

where we have fixed the constant by normalization and where $|n,n\rangle$ is the normalized state containing n excitations with momentum $\vec{k}$ and n with momentum $-\vec{k}$. Small changes in γ_+ will result in the following change in the state $|\Psi(\sigma)\rangle$

$$\begin{aligned}|\delta\Psi(\sigma)\rangle = \Bigg(&\frac{\gamma_+\delta\gamma_+^* + \gamma_+^*\delta\gamma_+}{\sqrt{1-|\gamma_+|^2}}\sum_{n=0}^{\infty}(\gamma_+)^n \\ &+\sqrt{1-|\gamma_+|^2}\sum_{n=0}^{\infty}n\,(\gamma_+)^{n-1}\,\delta\gamma_+\Bigg)\,|n,n\rangle\,.\end{aligned} \tag{56}$$

Evaluating the Fubini-Study line element

$$ds^2_{FS} = \langle\delta\psi|\delta\psi\rangle - \langle\delta\psi|\psi\rangle\langle\psi|\delta\psi\rangle\,, \tag{57}$$

results in

$$ds^2_{FS} = \frac{|\delta\gamma_+|^2}{(1-|\gamma_+|^2)^2}\,. \tag{58}$$

Restoring the continuum structure, including the momentum integrals and delta functions one reaches Eq. (44). Note that Vol/2 that appears there is the volume of the space of pairs of momenta.